Nuclear Instruments and Methods in Physics Research A 640 (2011) 85–90

Contents lists available at ScienceDirect

Nuclear Instruments and Methods in Physics Research A

journal homepage: www.elsevier.com/locate/nima

Performance of a new LMRPC prototype for the STAR MTD system

Y. Wang [a,*], H.S. Chen [a], W.C. Ding [a], X.Z. Qiu [a], J.B. Wang [a], X.L. Zhu [a], K.J. Kang [a], J.P. Cheng [a], Y.J. Li [a], L. Ruan [b], Z. Xu [b], K. Asselta [b], W. Christie [b], C. D'Agostino [b], J. Dunlop [b], J. Landgraf [b], T. Ljubicic [b], J. Scheblein [b], R. Soja [b], A.H. Tang [b], T. Ullrich [b], H.J. Crawford [c], J. Engelage [c], M. Calderon de la Barca Sanchez [d], R. Reed [d], H.D. Liu [d], J. Butterworth [e], G. Eppley [e], F. Geurts [e], W.J. Llope [e], D. McDonald [e], T. Nussbaum [e], J. Roberts [e], K. Xin [e], L. Bridges [e], J.C. Li [f], S. Qian [f], Z. Ning [f], H.F. Chen [g], B.C. Huang [g], C. Li [g], M. Shao [g], Y.J. Sun [g], Z.B. Tang [g], X.L. Wang [g], Y.C. Xu [g], Z.P. Zhang [g], H. Zeng [g], Y. Zhou [g], R. Clarke [h], S. Mioduszewski [h], A. Davila [i], G.W. Hoffmann [i], L. Li [i], C. Markert [i], L. Ray [i], J. Schambach [i], D. Thein [i], M. Wada [i], Z. Ahammed [j], P.P. Bhaduri [j], S. Chattopadhyay [j], A.K. Dubey [j], M.R. Dutt-Mazumdar [j], P. Ghosh [j], S.A. Khan [j], S. Muhuri [j], B. Mohanty [j], T.K. Nayak [j], S. Pal [j], R. Singaraju [j], V. Singhal [j], P. Tribedy [j], Y.P. Viyogi [j]

[a] Department of Engineering Physics, Tsinghua University, Beijing 100084, China
[b] Brookhaven National Laboratory, Upton, NY 11973, USA
[c] University of California, Berkeley, CA 94720, USA
[d] University of California, Davis, CA 95616, USA
[e] Rice University, Houston, TX 77251, USA
[f] Institute of High Energy Physics, CAS, Beijing 100049, China
[g] University of Science & Technology of China, Hefei 230026, China
[h] Texas A&M University, College Station, TX 77843, USA
[i] University of Texas, Austin, TX 78712, USA
[j] Variable Energy Cyclotron Centre, Kolkata 700064, India

ARTICLE INFO

Article history:
Received 12 December 2010
Received in revised form
28 January 2011
Accepted 7 March 2011
Available online 21 March 2011

Keywords:
MRPC
Time of flight
Wide strip
Beam test
Muon Telescope Detector

ABSTRACT

A new prototype of a Long-Strip Multi-Gap Resistive Plate Chamber (LMRPC) for the STAR Muon Telescope Detector (MTD) at RHIC has been developed. This prototype has an active area of 52×90 cm^2 and consists of six 250 μm wide gaps. Each detector has 12 strips, read-out at both ends, which are each 3.8 cm wide and 90 cm long with 0.6 cm intervals. In cosmic-ray tests, the efficiency was larger than 95% and the time resolution was ~75 ps for the 94% Freon, 5% iso-butane, and 1% SF_6 gas mixture. There was good uniformity in the performance across the different strips. The module was also tested in a proton beam at IHEP in Beijing. The efficiency was close to 100% and the best timing resolution achieved was 55 ps for the 90% Freon, 5% iso-butane, and 5% SF_6 gas mixture. Trigger scans along and across the strip direction were also performed.

1. Introduction

Multi-Gap Resistive Plate Chambers (MRPC) were introduced more than 10 years ago [1] as a new approach for accurate time-of-flight measurements. The technology is insensitive to magnetic fields, inexpensive and simple to build, and performs comparably or better than scintillators. Thus, MRPCs are now widely used in time-of-fight systems at medium and high energy physics experiments, such as the STAR experiment at the RHIC [2], the ALICE experiment at the LHC [3], and other experiments [4–6]. Data taken over the last several years have demonstrated that RHIC has created a dense and rapidly thermalized state of strongly interacting partonic matter [7]. The next objective at RHIC is to study the properties of this partonic matter in terms of the color degrees of freedom and the equation of state. The precise measurement of the transverse momentum distributions of quarkonia, such as the J/Ψ and Υ mesons, at different centralities in different collision systems and energies, serves as a thermometer of this partonic matter. A large-area and cost-effective Muon Telescope Detector (MTD) at mid-rapidity for

* Corresponding author. Tel.: +86 1062771960; fax: +86 1062782658.
E-mail address: yiwang@mail.tsinghua.edu.cn (Y. Wang).

0168-9002/$ - see front matter
doi:10.1016/j.nima.2011.03.012

the STAR has thus been proposed to improve STAR's capabilities at directly identifying the decay muons from quarkonia. Due to the low occupancy, the MTD will be constructed with the LMRPC technology instead of the smaller pad MRPCs used in the STAR time-of-flight system. With this design the number of electronic channels can be reduced and the hit position along a strip can be obtained by the time differences at the two ends of the strips. Prototypes of such LMRPCs have been running for the last three years in STAR [8,9] and many important results were obtained [10,11]. A new prototype with wider strips and fewer gaps was developed, which is more suitable for a large-area implementation of the MTD. In this paper, the design of these "final prototype" LMRPCs for the STAR MTD is presented. The results obtained from systematic cosmic-ray and beam tests are also discussed.

2. Structure of the module

A schematic side view of the detector structure is shown in Fig. 1. The module has six 250 μm wide gaps, which are defined by a stack of float glass plates separated by interleaved nylon monofilament fishing line. The inner and outer glass plates are 0.7 and 1.1 mm thick, respectively. The volume resistivity of the glass plates is about $10^{12}-10^{13}\,\Omega$ cm. The high voltage cathode and anode (HV electrodes) are a coating of colloidal graphite paint on the external surface of the outer glass plates. The graphite paint is applied by an automated sprayer at a constant speed, and the resulting surface resistance of the electrode is $\sim 5\,M\Omega/\square$. High voltage is applied to the electrodes via 10 mm wide and 800 mm long pieces of copper tape applied to the long edges of the painted electrodes. The active area of the module, which is defined by the stack of inner glass plates, is 52 cm × 90 cm. Twelve pairs of strips above and below the inner glass stack pick up the signals, which are each 3.8 cm wide and 90 cm long with 0.6 cm intervals between the strips. Mylar layers that are 0.18 mm thick are placed between the graphite paint and the printed circuit boards with the read-out strips to electrically insulate the HV electrodes and the read-out strips. Fiberglass-reinforced honeycomb plates mechanically support the device and keep it rigid.

Gas mixtures of primarily Freon R134A with admixtures of iso-butane and SF_6 are used as the working gas. The primary ionization created in the gas gaps following the traversal of a charged particle through the detector undergoes Townsend avalanche multiplication due to the high electric fields inside the gaps. The glass plates terminate the growth of the avalanches due to their high resistance. The movement of the avalanche electrons produces image charge signals in the pick-up pads. The total signals that are input to the front-end electronics (FEE) are the sum of all the avalanche signals in all the gas gaps. The outputs of FEE (the same FEE used for the STAR TOF prototype "TOFr" [12]) are digitized by VME based CAEN V792 (for charge) and CAEN 775E (for time).

3. Cosmic-ray test setup and results

Three 20 cm × 5 cm × 5 cm scintillators and two 4 cm × 2 cm × 1 cm scintillators were used to trigger on cosmic rays. The arrangement of the scintillators with respect to the LMRPC detector is shown in Fig. 2. Two of the larger scintillators and one of the smaller scintillators are above the module, and the rest are below the module. PMT0 through PMT4 was used for basic coincidence triggering and to provide the reference time. This same setup was used for the cosmic ray testing of the STAR TOF MRPC detectors [13]. Two small scintillators are used to measure the efficiency of the module—the width of the area subtended by the small scintillators is smaller than the width of an LMRPC strip.

The performance of the LMRPC module when using two different gas mixtures was investigated. One gas mixture consisted of 95% Freon and 5% iso-butane, while the other consisted of 94% Freon, 5% iso-butane, and 1% SF_6. For each gas mixture, the detector efficiency, time resolution, and noise rates were measured.

The plots of efficiency and time resolution versus the electric field, E, in the gas gaps are shown in Fig. 3. The electric field, E, is equal to the applied HV (total voltage drop between HV anode and cathode) divided by the total thickness of the gas gaps (6×0.025 cm). An efficiency higher than 95% was achieved at electric field values of 96.3 kV/cm (applied HV of ± 7.22 kV) for the 95% Freon plus 5% iso-butane mixture, and at 98.3 kV/cm (applied HV of ± 7.37 kV) for the 94% Freon, 5% iso-butane, plus 1% SF_6 mixture. The time resolution values are shown on the right axis of Fig. 3. These were 95–100 ps for the 95% Freon plus 5% iso-butane mixture and 75–80 ps for the 94% Freon, 5% iso-butane, plus 1% SF_6 mixture.

The plots of noise rates versus the electric field values are shown in Fig. 4 for the 94% Freon, 5% iso-butane, plus 1% SF_6 mixture.

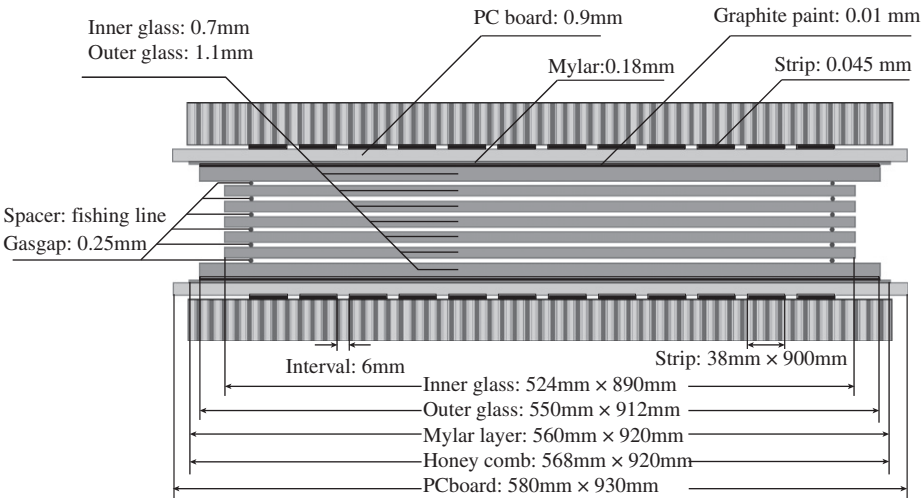

Fig. 1. Structure of the LMRPC module.

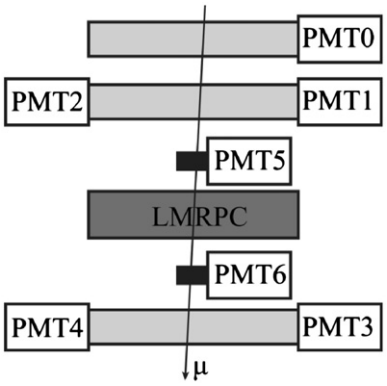

Fig. 2. Layout of the cosmic-ray test system.

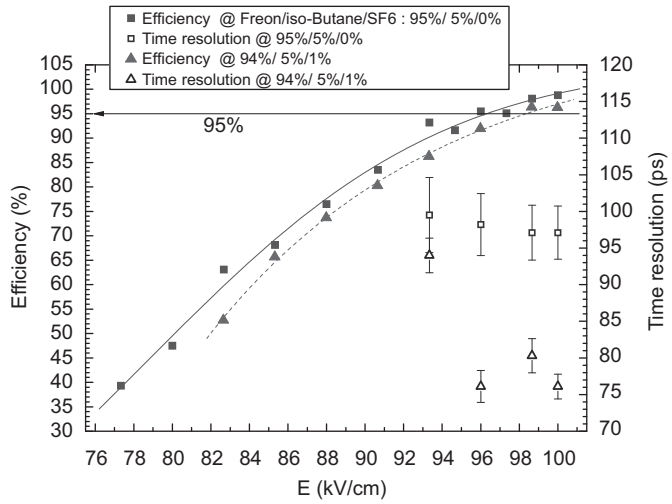

Fig. 3. Efficiency and time resolution versus the electric field for both gas mixtures.

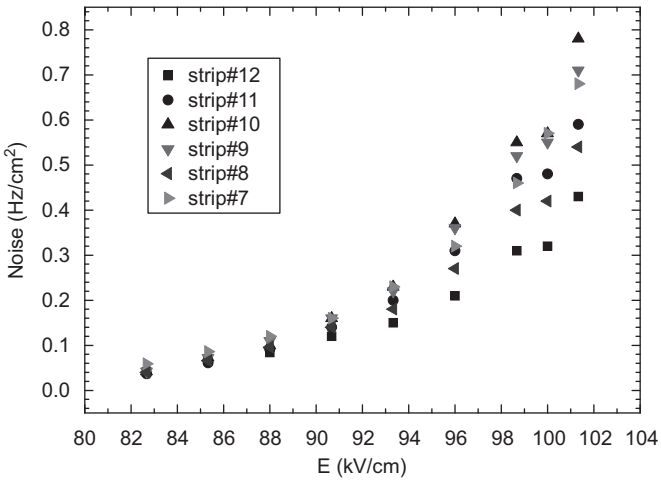

Fig. 4. Noise levels on strips #7 through #12 as a function of the electric field for the 94% Freon, 5% iso-butane, and 1% SF_6 gas mixture.

The values are less than 0.4 Hz/cm^2 when the electric field is smaller than 96 kV/cm (applied HV of $\pm$7.2 kV). The noise level versus the strip number for an electric field of 104 kV/cm (applied HV of $\pm$7.8 kV) is shown in Fig. 5. The noise rate is relatively stable and ranges from 0.6 to 1.0 Hz/cm^2, implying a good uniformity of the device across the different strips.

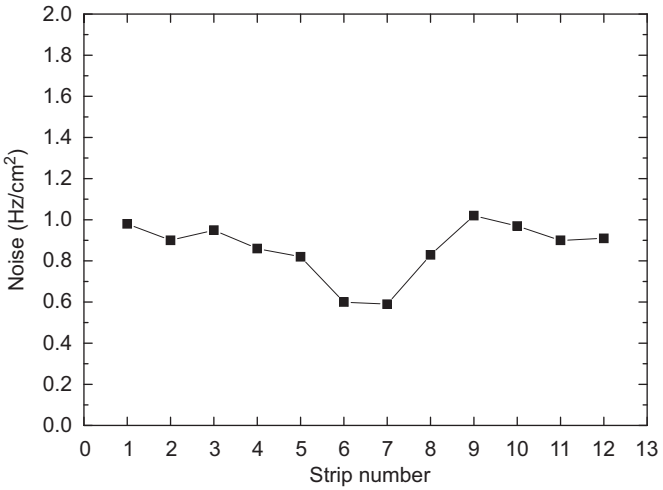

Fig. 5. Noise levels versus the strip number for the electric field of 104 kV/cm and the 94% Freon, 5% iso-butane, and 1% SF_6 gas mixture.

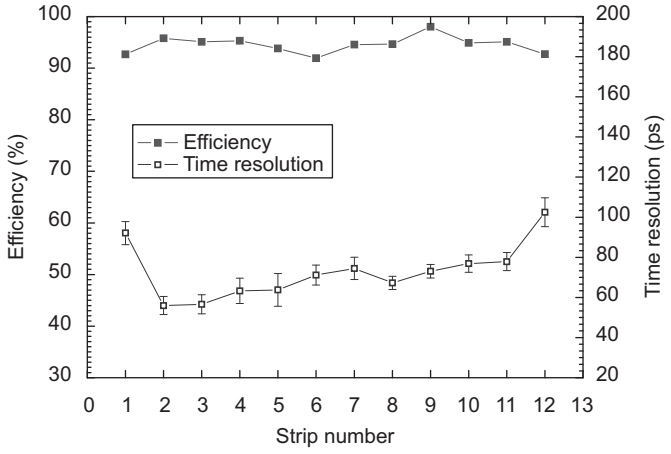

Fig. 6. Efficiency (solid squares) and time resolution (open squares) versus the strip number for a 96 kV/cm electric field and the 94% Freon, 5% iso-butane, and 1% SF_6 gas mixture.

The uniformity across the different strips was also tested for the electric field of 100 kV/cm (applied HV of $\pm$7.5 kV) for the 94% Freon, 5% iso-butane, and 1% SF_6 gas mixture. The trigger scintillators were placed over each of the different LMRPC strips in turn. The efficiency and the time resolution of each strip are shown in Fig. 6. The uniformity of the different strips is good. The efficiency is approximately 95% and the time resolution ranges from 60 to 80 ps. A non-uniformity of the electric field near the two outermost strips results in a somewhat degraded, but still acceptable, time resolution for those two strips.

4. Beam test at IHEP

4.1. Detectors layout

The module was also tested in beam at the Institute of High Energy Physics (IHEP), CAS in Beijing. The experimental area was located at the end of the E3 line in experiment Hall number 10. A schematic depiction of the detector configuration is shown in Fig. 7. Two scintillators (SC1 and SC2) and a Cherenkov detector (C0) were used for basic triggering. A coincidence of the two

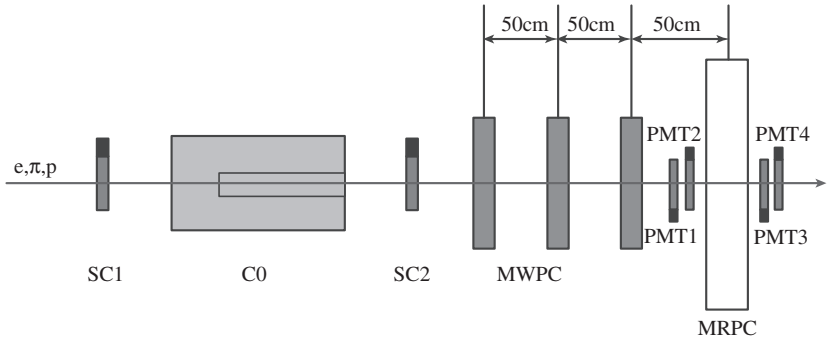

Fig. 7. Schematic view of the detectors used for the beam tests of the LMRPC.

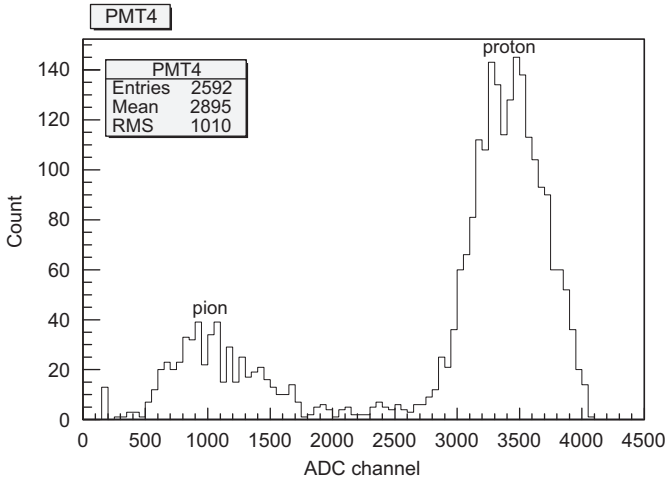

Fig. 8. Typical charge spectrum of PMT4. Peaks resulting from pion and proton beam particles are well separated.

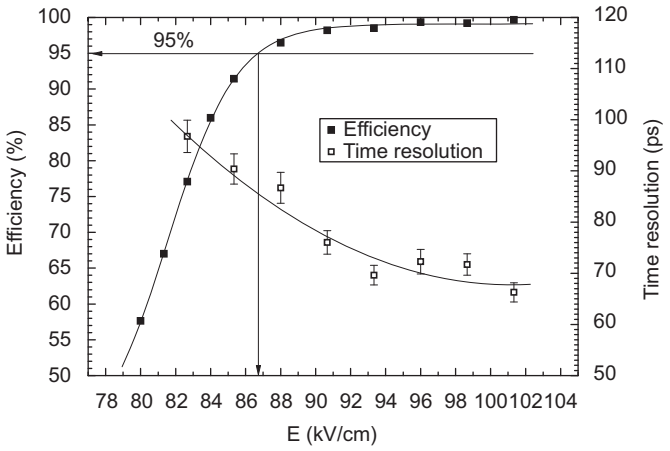

Fig. 9. Efficiency (solid squares) and time resolution (open squares) versus the electric field.

scintillators and an (anti)coincidence with the Cherenkov detector allowed the selection of protons and pions [14]. Three multi-wire chambers (MWPC) were installed for the measurement of the beam trajectory and the hit positions on the LMRPC but these detectors were inoperable during the beam time. The four small scintillators (PMT1-4) provided the coincidence trigger and the event reference time (T0), and these were the same four detectors that were used in the cosmic ray testing described above. The LMRPC was placed in a movable platform with a range of ± 20 cm horizontally and ± 5 cm vertically. The gas mixture used was 90% Freon, 5% iso-butane, and 5% SF_6.

4.2. Particle selection

It was not possible to directly identify the incident beam as protons and pions at the 600 MeV/c beam momentum using the SC1, SC2, and C0 detectors. However, the very different ionization energy loss of these two particles in plastic allowed a direct identification of the beam particle by the T0 detectors PMT1–PMT4. A typical charge spectrum of PMT4 is shown in Fig. 8. The two peaks formed by pion and proton beam particles are well separated. Protons were selected in the offline analysis due to their higher beam rate. There are differences on the efficiency, time resolution, and other performance because low-energy protons ionize approximately two times more than pions (the energy depositions in the gas mixture in the LMRPC module of 600 MeV/c proton and pion are 8.6×10^{-4} and 3.8×10^{-4} MeV, respectively, simulated by GEANT4).

4.3. HV scan

A wide-range HV scan was done, and the result is shown in Fig. 9. The efficiency reached 95% when the electric field was $\sim$87 kV/cm (applied HV of $\pm$6.525 kV) and was nearly 100% for a wide range of working electric fields (90–100 kV/cm). Within this range of applied high voltage values, the time resolution was around 70 ps. Compared with the result of cosmic-ray test, the curves of efficiency reach the plateau region at lower values of the electric field. That is because the protons used in the beam test were more strongly ionizing compared to cosmic-ray particles. The charge spectrum from the LMRPC module for an electric field of 96 kV/cm is shown in Fig. 10. A distinct high-charge peak from "streamers" was not observed.

4.4. Trigger scan

The LMRPC module can be moved horizontally and vertically using the movable platform. A vertical trigger scan was done at an electric field of 96 kV/cm. The trigger moved in steps of 0.5 cm. The efficiency of the nearest two strips to the beam, and the "AND" and "OR" efficiencies as a function of the central position of trigger, is shown in Fig. 11. Like a typical trigger scan efficiency profile (see e.g. Refs. [15,16]), the efficiency of a strip decreases when the triggered spot is moved away from the strip. The "AND" efficiency (the charge sharing and strip-to-strip cross-talk) is maximal when the trigger spot is near a strip-to-strip gap, while the "OR" efficiency remains high with only a small decrease near the gap. The time resolution at each of these same positions is

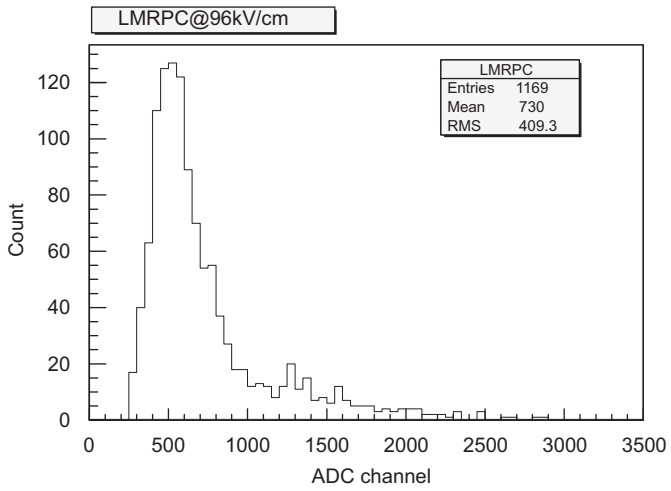

Fig. 10. Charge spectrum from the LMRPC for an electric field of 96 kV/cm.

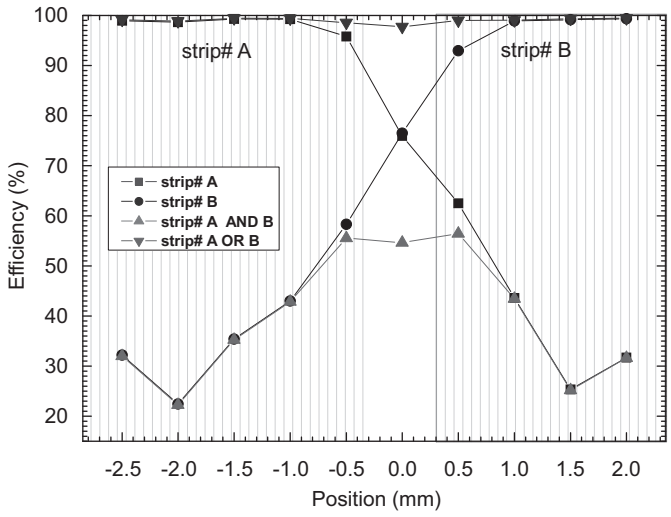

Fig. 11. Efficiency of the module while moving the trigger vertically across different strips.

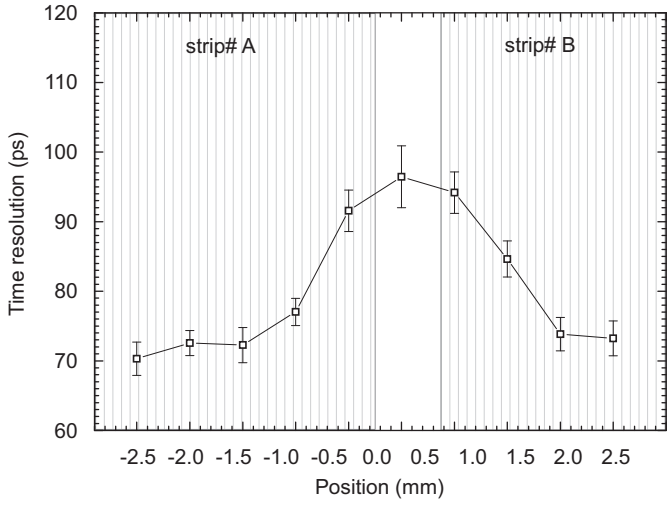

Fig. 12. Time resolution of the module while moving the trigger vertically across different strips.

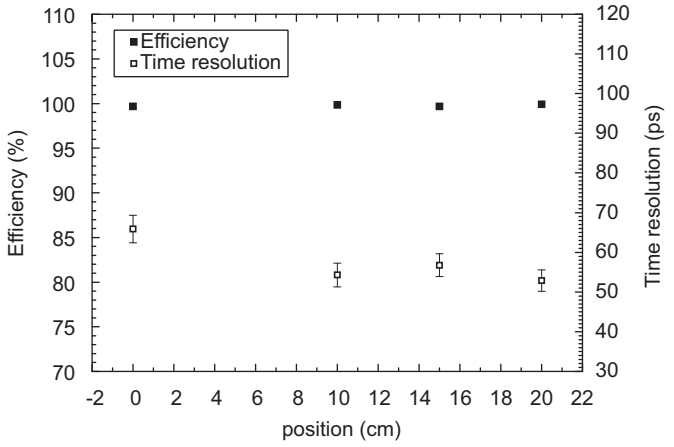

Fig. 13. Efficiency and time resolution of the module while moving the trigger spot horizontally along a strip.

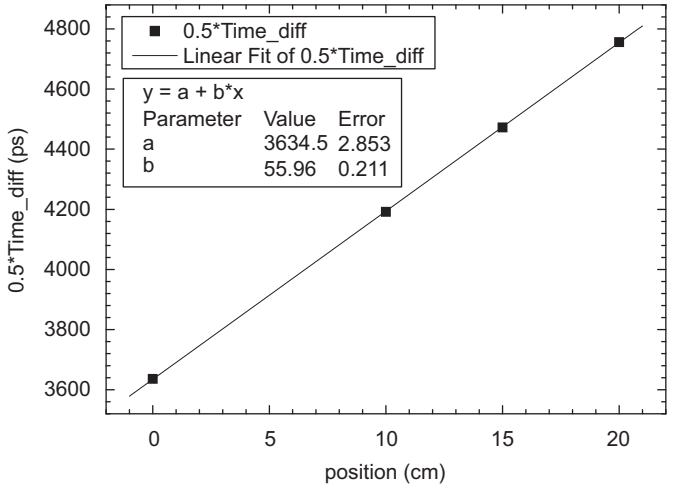

Fig. 14. Time difference of the signals from the two ends of one strip (Δt) versus the position of the trigger spot (D). The relationship between these two parameters is $\Delta t/2 = D/v + t_0$. The propagation velocity of the signal is $v = 55.96 \pm 0.21$ ps/cm.

shown in Fig. 12. The time resolution degrades from ~75 to ~95 ps for hits near the gap.

A trigger scan along the long axis of the strips was also done. The trigger spot was moved in steps of 5 cm each, and three different positions were tested. The plot of efficiency and time resolution versus the position along the strip is shown in Fig. 13. A good uniformity along the strip is observed. The efficiency was close to 100% and the time resolution ~55 ps. The propagation velocity of the signal along the strip was calculated via the time difference at the two ends of the strip. The resulting propagation speed of the signals inside the pads was observed to be ~56 ps/cm, as shown in Fig. 14.

5. Conclusions

A new prototype of a LMRPC detector for the STAR MTD has been built and tested. The active area is $52 \times 90\ \text{cm}^2$ and is read out by twelve $3.8 \times 90\ \text{cm}^2$ double-ended strips. The performance for timing resolution and efficiency in cosmic ray and beam tests was good, and the performance was uniform across the different

read-out channels. In the cosmic ray tests, the efficiency was higher than 95% and the time resolution was around 75 ps. In the beam tests (with a different gas mixture) the efficiency was nearly 100% and the time resolution was as good as 55 ps. The test results also show a good uniform performance across the different strips and along the strip.

This new prototype meets the basic requirements for the STAR MTD. Three of these detectors will be installed in STAR and will be operated throughout the upcoming 2011 run.

Acknowledgments

The authors thank the IHEP test beam group for providing the excellent beam and the necessary equipment. This work is supported by the National Natural Science Foundation of China under Grant nos. 11020101059, 10775082, 11050110111, and 10979030.

References

[1] E. CerronZeballos, et al., Nucl. Instr. and Meth. A374 (1996) 132.
[2] 〈http://wjllope.rice.edu/∼TOF/TOF/Documents/TOF_20040524.pdf〉 (accessed on 18.11.2010).
[3] ALICE Time of Flight Addendum, CERN/LHCC 2002-016, Addendum to ALICE TDR 8, 24 April 2002.
[4] A. Schüttauf, et al., Nucl. Instr. and Meth. A 533 (2004) 65.
[5] H. Alvarez-Pol, et al., Nucl. Instr. and Meth. A 535 (2004) 277.
[6] V. Ammosov, et al., Nucl. Instr. and Meth. A 578 (2007) 119.
[7] J. Adams, et al., Nucl. Phys. A 757 (2005) 102.
[8] Y. Sun, et al., Nucl. Instr. and Meth. A 593 (2008) 307.
[9] Xiaobin Wang, Chin. Phys. C 33 (2) (2009) 114.
[10] L Ruan, J. Phys. G: Nucl. Part. Phys. 36 (2009) 095001 (15 pp.).
[11] L. Ruan, et al., STAR Muon Telescope Detector Proposal: 〈http://drupal.star.bnl.gov/STAR/system/files/MTD_proposal_v14.pdf〉.
[12] F. Geurts, et al., Nucl. Instr. and Meth. A 533 (2004) 60.
[13] Y. Wang, et al., Nucl. Instr. and Meth. A 613 (2010) 200.
[14] Jia-Cai Li, et al., HEP & NP 28 (2004) 1269.
[15] A. Blanco, et al., Nucl. Instr. and Meth. A 485 (2002) 328.
[16] D. Gonzalez-Diaz, Nucl. Instr. and Meth. A, in press, 10.1016/j.nima.2010.09.067.